Antibacterial Activity of Highly Porous Vinyl alcohol group containing Polymer/MWNT Nanocomposite Particles

Kyu Ryn Kim[1], **Hyun Jeong Jeon**[2], **Eun-Ju Lee**[3] and **Eun-Soo Park**[4]

[1] YBRAIN Inc., B1, Sae-Rom Bldg., 551, Seolleung-ro, Gangnam-gu, Seoul 135-916, Korea
[2] Department of Green Life Science, Sangmyung University, Seoul 110-743, Korea
[3] Advanced Material Development Team, Korea Engineering Plastics Co., Ltd., SK Ventium Bldg 104(2F), 166, Gosan-ro, Gunpo-si, Gyeonggi-do, 435-776, Korea
[4] Green Energy and Material Team, Young Chang Silicone Co., Ltd., (Gasan-dong) 205-16, Gasandigital 1-ro, Geumcheon-gu, Seoul 153-803, Korea

The interest in polymer nanocomposites with antimicrobial properties is continuously increasing due to the growing demand for healthy living. More and more such materials are produced using different technologies in order to achieve desired properties. Potential fields of application include, for instance, textile, industrial and food packaging or medical devices to prevent nosocomial infections. The aim of this study is to investigate new antibacterial polymer nanocomposites using electron-beam irradiated multi-walled carbon nanotube (EB-MWNT) by simple saponification method and compare their antibacterial activity depending on polymer matrix and saponification time. Polyvinyl acetate (PVAc) and poly(ethylene-*co*-vinyl acetate) [VAc content = 28 % (EVA28) and 40 % (EVA40)] are each dissolved in toluene and EB-MWNT was dispersed in polymer solution. Followed by the suspension was precipitated and saponified in alkaline non-solvent. Morphology, thermal properties and antibacterial activity of the prepared nanocomposite particles have been evaluated.

Keywords: microbial; nanocomposites; electron beam irradiation; copolymer; morphology; carbon nanotube

1. Introduction

Concerns about contagious spread of infection are growing. This is particularly remarkable because many infectious diseases spread via direct surface contact with contaminated materials [1]. Many pathogens in the biofilms mode of growth on various surfaces usually evolve as persistent transmission sources because of their highly inherent resistance to antimicrobial agents [2, 3]. Antimicrobial materials are thus desired and their widespread application can be anticipated [3-9]. Various field of practical usage includes aerospace, defence, biomedical devices, food and pharmaceutical processing and packaging industries as well as the public transportation system. Polymers with antimicrobial activity are often required for food packaging, sanitary, or medical application. They can also be used as a coating material for common objects such as doorknobs, children's toys, and computer keyboards to prevent transmission of microbial infections. They have usually been prepared by compounding antimicrobial agents into ordinary synthetic polymers [6].

The interest in polymer nanocomposites exhibiting antimicrobial activity is continuously increasing due to the growing demand for healthy living. Carbon nanotubes (CNTs) are some of the most attractive nanomaterials because of their unusual physicochemical, mechanical, and electrical properties as well as their broad range of potential applications. The increase in commercial interest and subsequent mass production will lead to greater possibilities for interactions of CNTs with humans and the environment [10]. Recently, Kang and coworkers reported that CNTs possess antimicrobial properties themselves, and their relevant activities were ascribed to the behavior of 'nanodart' with the proposed physical damage mechanism [11]. The intrinsic toxicity of CNT depends on the degree of surface functionalization and the different toxicity of functional groups. In this study, poly(vinyl alcohol) (PVOH)/MWNT and poly(ethylene-*co*-vinyl alcohol) (EVOH)/MWNT porous nanocomposite particles were prepared from PVAc/MWNT/toluene and EVA/MWNT/toluene suspensions, respectively using precipitation and alkaline saponification. The MWNT was functionalized electron beam (EB) irradiation process in air. Morphology, mechanical properties and antibacterial activity of the prepared porous nanocomposite particles has been evaluated.

2. Experimental

2.1 Materials

MWNT [CM-95 (purity: 95 wt%; diameter: 15 nm; length: 20 μm; specific gravity: 1.8), Iljin CNT, Korea], PVAc (189480, Mw ≈ 100,000, Sigma-Aldirich, MO, USA), EVA28 [1159 (density: 0.949, vinyl acetate content: 28 wt%, melt flow index: 18 g/10 min (190 °C/2,16 kg)), Hanhwa Chemical Co., Ltd., Seoul, Korea], and EVA40 [340502 (density: 0.941, vinyl acetate content: 40 wt%, melt flow index: 57 g/10 min (190 °C/2,16 kg), Sigma-Aldirich, MO, USA] was used as received. EVA resin and MWNT was pre-dried in a vacuum drying oven for at least 12 h at 40 °C to

remove any moisture from the pellets before processing. The MWNT were EB irradiated in air at room temperature using an EB accelerator [ELV 4 (Energy: 0.8 ~ 1.5 MeV, EB power: 50 kW, Non-uniformity of Current density: < 10 %, Input voltage: 220/380)], EB tech Co., Ltd., Daejeon, Korea].

2.2 Instrumentation

Scanning electron microscopy (SEM) observations of the samples were performed on a Hitachi S-4300 model (Tokyo, Japan). The fractured surfaces of the nanocomposites were prepared by using cryogenic fracturing in liquid nitrogen followed by a coating with platinum in an SPI sputter coater. The morphology was determined using an accelerating voltage of 15 kV. The surface sample composition was evaluated using SEM (Hitachi S-4300 model, Tokyo, Japan) equipped with an energy dispersive X-ray spectroscopy (EDX). The transmission scanning microscopy (TEM) measurements were performed with a Philips CM200 operated at 200 kV. Film specimens were prepared by pressing the composites on a hot press at a plate press at 150 - 250 °C for 10 min under about 5 atm and quickly immersed into water. The sheet thus formed was free from any distortion problems. The films obtained were allowed to dry at 60 °C for 24 h. The final thickness of the dried films was in the range of 0.2 - 0.4 mm. Dumbbell specimens for tensile tests were prepared in accordance with IEC 60811-1-1 specification. Tensile properties of samples were determined with a universal test machine (UTM, Model DEC-A500TC, Dawha test machine, Korea) at a cross head speed of 250 mm/min. The mean value of at least five specimens of each sample was taken, although specimens that broke in an unusual manner were disregarded.

2.3 Preparing of PVAc/MWNT and EVA/MWNT nanocomposite particles

PVAc/MWNT and EVA/MWNT nanocomposites were prepared with nanotube loadings of 10 wt%. The polymer pellets (100 g) were first swelled in toluene (900 g) at room temperature for 12 h and followed by heating at 60 °C for 4 h. The MWNT (1 g) was dispersed in EVA/toluene solution (90 g) [toluene: 81 g, polymer: 9 g, MWNT: 1 g] by mechanical premixing and bath sonication for 2 h. 20 ml of diluted PVAc/MWNT/toluene (or EVA/MWNT/toluene) suspension (2.50 wt% in toluene) was saponification by dropwise addition to 200 ml of 0.5 M KOH in ethanol (or methanol) solution. The heterogeneous suspension was stirred at room temperature for 6 h, and then the suspension was filtrated, and filtrate washed with methanol. The filtrate was dried under vacuum at 60 °C to a constant weight. The percent saponification of the EVA was determined from Fourier transform infrared (FTIR) absorbance ratio of methyl group of vinyl acetate unit (1370 cm^{-1}) and the methylene group of the ethylene unit (720 cm^{-1}) [12]

2.4 Shake flask test

The antibacterial activity of the nanocomposite powders was tested against *Staphylococcus aureus* (*S. aureus*, ATCC 25923) and *Escherichia coli* (*E. coli*, ATCC 25922) with the shake flask method. The bacteria were subcultured on nutrient broth and incubated for 20 h at 37 °C. The cells were suspended in 50 ml of phosphate-buffered saline (PBS) to yield a bacterial suspension of 7.00×10^8 - 2.49×10^9 colony forming units/ml (cfu/ml). The sample powder (1 g) was weighed and shaken in 20 ml of a bacterial suspension for 24 h. The suspension (50 wt/vol%) was serially diluted in PBS and cultured on nutrient broth at 37 °C for 24 h. The number of viable organisms in the suspension was determined by multiplication of the number of colonies with the dilution factor, and the percentage reduction was calculated on the basis of the initial count

3. Results and Discussion

3.1 EB irradiation effect of MWNT

Figure 1 shows the TEM image and EDX result of MWNT produced by a chemical vapour deposition (CVD) process without any purification. As-received MWNT contain some impurities and entangle into a bulk piece (Figure 1a). EDX results of the pristine MWNT show small peaks which are corresponding to Fe, Si and S (Figure 1b). The Si peak has its origin in silicon substrate whereas the other peaks are due to the precursor gases present in the gas mixture and catalyst. The Pt peaks was due to the platinum sputtering process during sample preparation. CNTs are often formed in entangled ropes with 10 - 100 CNTs per bundle depending on the method of synthesis. They can be produced by a number of methods: direct-current arc discharge, laser ablation, thermal and plasma enhanced CVD process [13]. The method of production affects the level of purity of the sample and whether SWNTs or MWNTs are formed. Impurities exist as catalysis particles, amorphous carbons and non-tubular fullerenes [14]. The MWNT were EB-irradiated in air at room temperature using a 1.5 MeV electrostatic accelerator. Irradiation dose of 800, 1000, and 1200 kGy were used.

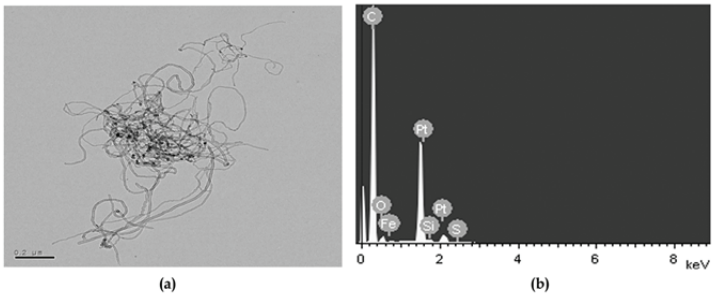

Fig. 1 SEM images (a) and EDX analysis (b) result of the pristine MWNT.

The pristine MWNT has relatively smooth surface without extra phase or stain attached on its sidewall. Although the EB irradiation increased up to 800 kGy, the surface appearance little changed compare to the pristine MWNT. After the 1200 kGy EB irradiation, the smooth surface was disappeared, many wrinkled structure were formed, and the surface roughness increased. Additional sample characterization is carried out using TEM. From the Figure 2, the presence of dark spots on the outer wall of the MWNT1200 suggests that damage and formation change of MWNT induced by high-dose irradiation. In general, the surface of the synthesized CNT is smooth and relatively defects free. However, stresses can induce Stone-Wales transformations, resulting in the formation of heptagons and concave areas of deformation on the nanotubes [14, 15]. Moreover EB irradiation of MWNTs resulted in forming vacancies on their walls and eventual amorphization upon high-dose irradiation [16]. The irradiation induced damage manifested itself in the deterioration of mechanical properties of MWNTs exposed to prolonged 2 MeV EB irradiation [17].

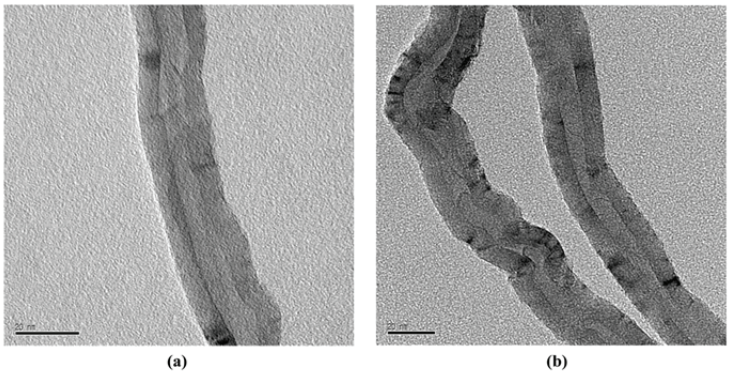

Fig. 2 TEM image of the MWNT before (a) and after (b) EB irradiation at 1200 kGy.

Elemental analyses (EA) results of the MWNT and EB-MWNT are shown in Table 1. EA was performed in a Thermo EA1112 apparatus. The results presented a decrease in the hydrogen content up to 1000 kGy. After the 1200 kGy irradiation, the hydrogen content was significantly increased. This indicated that the low irradiation dose cleaned the MWNT surface of impurities, according to the SEM, EDX and EA results, but the increase in the irradiation doses could have affected the surface roughness and chemical composition [18].

Table 1 EA results of the pristine MWNT and EB-MWNT [18].

Element	Composition (%)			
	MWNT	MWNT800	MWNT1000	MWNT1200
C	99.50	99.52	99.52	99.35
H	0.50	0.48	0.48	0.57
N	-	-	-	0.08

3.2 Porous structure of saponified PVAc/MWNT and EVA/MWNT nanocomposites

PVAc/MWNT1200, EVA40/MWNT1200 and EVA28/MWNT1200 are each dissolved in toluene and MWNT was dispersed in polymer solution. Followed by the polymer suspension was precipitated and saponified in alkaline non-solvent. After rinsing off the coagulant and drying, sponge-like structure of connected matrix polymer and MWNT were obtained. This causes separation of the heterogeneous polymer suspension into a solid nanocomposite and liquid solvent phase. The approximate size of the saponified particles is 30 - 50 μm.

Figure 3 shows surface of PVAc/MWNT1200 and EVA/MWNT1200 coagulant before and after 6h-saponification time. The surface of the EVA28/MWNT1200 coagulant (Figure 3c) shows a relatively dense skin layer comparing to

PVAc/MWNT1200 (Figure 3a) and EVA40/MWNT1200 (Figure 3b) ones. Small pores can be seen on the surface of the coagulants. The formation of the skin layer and lack of an interconnected pore structure is likely due to the rapid precipitation where the rate of inter-diffusion depends on the value of the solubility parameters of the solvent and non-solvent. In sharp contrast, PVAc/MWNT1200 and EVA40/MWNT1200 coagulants show a fibrous structure composed of polymer matrix and MWNT fibrils. As the saponification time increase, the PVAc/MWNT1200, EVA40/MWNT1200 and EVA28/MWNT1200 nanocomposites form a porous structure containing a network of open-cell pores at the nanometer length scale. The pore size was obtained directly by image analysis from higher magnification SEM micrographs. The pore sizes of 6 h saponified EVA/EB-MWNT ranged between 50 and 200 nm. At low polymer/MWNT suspension concentrations, the particles were less porous and the precipitated polymer phase had a granular structure consisting of aggregates of precipitated polymer micelles. While at high concentrations, void porosity was increased and the precipitated polymer phase became a spongy-like structure [18]. It was also found that as VAc content was increased, the average pore size was decreased.

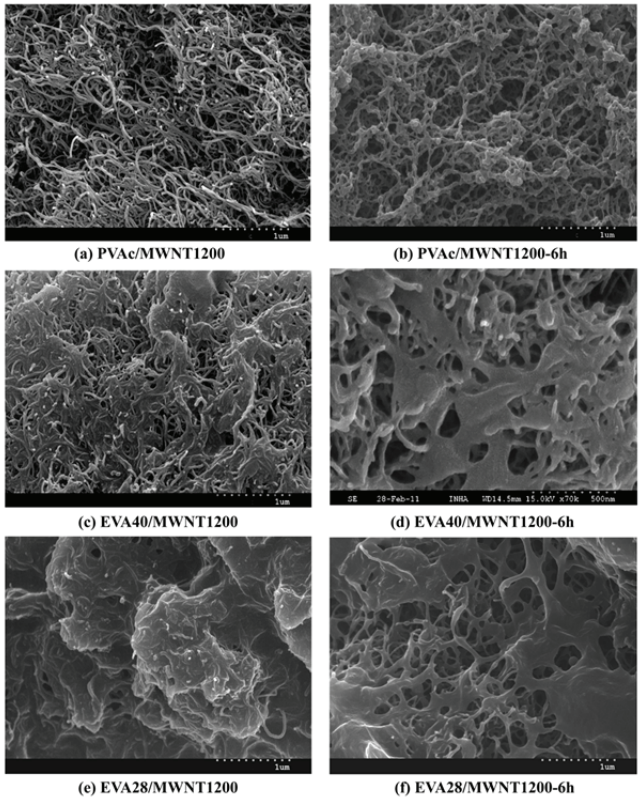

Fig. 3 SEM images of the nanocomposite particle before and after 6h-saponification time (polymer/MWNT = 90/10 wt%, Fig.3e and 3f [19]).

3.3 Mechanical properties of saponified PVAc/MWNT and EVA/MWNT nanocomposites

Table 2 demonstrates the tensile properties of the PVAc/MWNT1200, EVA40/MWNT1200 and EVA28/MWNT1200 nanocomposites. Addition of 10 wt% of MWNT1200 enhances the tensile strength of EVA40 and EVA28 by 25 % and 18.9 %, respectively whereas the tensile strength of PVAc decreases by 18.8 %. In sharp contrast the elongation at break of EVA40/MWNT1200 and EVA28/MWNT1200 nanocomposites decreased with the presence of filler that indicates interference by the filler in the mobility or deformability of the matrix [18]. An increase in weight percentage of filler reduced the deformability of the matrix, and, in turn, reducing the ductility in the skin area so that the composite tended to form a weak structure. The tensile strength and elongation at break of EVA40/MWNT1200 and EVA28/MWNT1200 were significantly increased with saponification time. At 6h-saponification time, the tensile strength of EVA40/MWNT1200 nanocomposite was increased by 2.8-fold to 32.3 MPa whereas EVA28/MWNT1200 increased the tensile strength by 1.7-fold to 21.5 MPa as compared to the un-saponified one. The elongation at break of the both nanocomposite also increased by 1.6-fold and 5.2-fold, respectively. The tensile strength of PVAc/MWNT1200 nanocomposite significantly increased with saponification time. After 6h-saponification time, it enhanced by 222 %. However, the elongation at break of the PVAc/MWNT1200 almost remained same or has raised only maringally. This is indicated that saponification process enhances the overall dispersion state of the MWNT due to enhanced interactions between the filler and the polymer matrix.

Table 2 Tensile properties of the saponified EVA/MWNT and PVAc/MWNT nanocomposites.

Sample	Tensile properties	
	Tensile strength (MPa)	Elongation at break (%)
PVAc	22.9 ± 2	5 ± 0
PVAc/MWNT1200	18.6 ± 1	4 ± 1
PVAc/MWNT1200-1h	26.3 ± 5	4 ± 1
PVAc/MWNT1200-3h	33.4 ± 5	5 ± 1
PVAc/MWNT1200-6h	37.7 ± 8	8 ± 4
EVA40	9.2 ± 1	1,604 ±182
EVA40/MWNT1200	11.5 ± 1	537 ± 38
EVA40/MWNT1200-1h	12.1 ± 1	781 ± 36
EVA40/MWNT1200-3h	22.8 ± 4	826 ± 54
EVA40/MWNT1200-6h	32.3 ± 6	851 ± 60
EVA28	10.6 ± 1	1,472 ± 106
EVA28/MWNT1200	12.6 ± 1	184 ± 27
EVA28/MWNT1200-1h	16.5 ± 4	880 ± 75
EVA28/MWNT1200-3h	18.6 ± 1	982 ± 58
EVA28/MWNT1200-6h	21.5 ± 2	950 ± 66

3.4 Antibacterial activity of EB-MWNT

The antibacterial activity of the pristine MWNT and EB-MWNT was compared against *S. aureus* and *E. coli* with the shake flask method. The number of viable bacteria and the percentage reduction of the number of bacteria are summarized in Table 3. After 24 h of bacterial contact, pristine MWNT extirpated 8.2 and 10.3 % of the viable cells of *S. aureus* and *E. coil*, respectively. This indicated that pristine MWNT has some interesting biological activities.

With the EB irradiation dose the biological activity of MWNT against both the *S. aureus* and *E. coil* was gradually increased. It is noteworthy that 1200 kGy irradiated MWNT exhibits highest antibacterial activity against *S. aureus* and *E. coil*. After 24 h of shaking, MWNT1200 showed 28.9 and 33.2 % inhibition of the growth of *S. aureus* and *E. coil*., respectively. Harmful effect of nanoparticles arises due to high surface area and intrinsic toxicity of the surface. The nano-scale dimensions of CNT make quantities of milligrams possess a large number of cylindrical particles with a concurrent very high total surface area. In addition the intrinsic toxicity of CNT depends on the degree of surface functionalization and the different toxicity of functional groups. Batches of pristine CNT readily after synthesis contain impurities such as amorphous carbon and metallic catalysts which can also be the source of toxic effects [20]. Kang and coworkers [11] showed that the size of CNTs is a key factor governing their antibacterial effects and that the likely main CNT-cytotoxicity mechanism is cell membrane damage by direct contact with CNTs. As the size of CNTs decreases, the specific surface area increases, leading to increased opportunity for interaction and uptake by living cells. This characteristic could result in adverse biological effects that otherwise would not be possible with the same material in a larger form [21-22]. Several studies have shown that SWNTs exhibit significant cytotoxicity to human and animal cells, whereas MWNTs exhibit a milder toxicity [22].

Table 3 Shake flask test results for the pristine MWNT and EB-MWNT [19].

Sample	Antibacterial activity (50 wt/vol%)			
	S. aureus		*E. coil*	
	cfu/ml ($\times 10^{-9}$)	Reduction (%)	cfu/ml ($\times 10^{-9}$)	Reduction (%)
Blank	2.32	-	2.49	-
MWNT	2.13	8.2	2.08	10.3
MWNT800	1.85	20.3	1.93	16.8
MWNT1000	1.72	25.9	1.78	23.3
MWNT1200	1.65	28.9	1.55	33.2

3.6 Antibacterial activity of porous nanocomposite particle

The number of viable bacteria and the percentage reduction of the number of bacteria for prepared porous particles are summarized in Table 4 and the percentage reductions are compared in Figure 4. It is curious to observe that the EVA40 and EVA28 displayed some antimicrobial activity against both Gram-positive *S. aureus* and Gram-negative *E. coli*, whereas the PVAc exhibited activity toward *E. coli*. From the Figure 4, the PVA/MWNT1200, EVA40/MWNT1200 and EVA28/MWNT1200 nanocomposites showed improved antibacterial activity against *S. aureus* and *E. coli* as compared with the corresponding unfilled ones. The incorporation of 10 wt% MWNT1200 into PVAc, EVA40 and EVA28 matrix resulted in 86, 32 and 690 % increase in antibacterial activity against *E. coil*, respectively. While this addition led to 135, 17 and 84 % increase in activity against *S. aureus*. Based on the above, the increase in antibacterial

activity is assumed to be due to the increase in intrinsic toxicity generated from the surface functionalized MWNT by EB irradiation.

Table 4 Antibacterial activity of the nanocomposite particles.

Sample	Antibacterial activity (50 wt/vol%)			
	S. aureus		*E. coil*	
	cfu/ml ($\times 10^{-8}$)	Reduction (%)	cfu/ml ($\times 10^{-8}$)	Reduction (%)
Blank	7.10	-	12.4	-
PVAc	9.40	-32.4	1.03	16.9
PVAc/MWNT1200	6.30	11.3	8.50	31.5
PVAc/MWNT1200-1h	4.20	40.8	3.80	69.4
PVAc/MWNT1200-3h	4.10	42.3	2.60	79.0
PVAc/MWNT1200-6h	2.70	62.0	2.10	83.1
Blank	15.3	-	12.4	-
EVA40	10.6	30.7	7.40	40.3
EVA40/MWNT1200	9.81	35.8	5.80	53.2
EVA40/MWNT1200-1h	7.80	49.0	4.40	64.5
EVA40/MWNT1200-3h	5.20	66.0	3.50	71.8
EVA40/MWNT1200-6h	2.90	81.0	0.50	96.0
Blank	15.3	-	10.0	-
EVA28	10.4	32.0	9.00	10.0
EVA28/MWNT1200	6.30	58.8	2.10	79.0
EVA28/MWNT1200-1h	5.60	63.4	1.85	81.5
EVA28/MWNT1200-3h	5.20	66.0	1.80	82.0
EVA28/MWNT1200-6h	5.00	67.3	1.40	86.0

Similarly the antibacterial activity against both bacterial strains of all nanocomposites was gradually increased with the saponification time. The EVA40/MWNT1200-6h exhibited highest antibacterial activity against two strains. After 24 h of shaking, it showed 81 and 96 % inhibitions of the growth of *S. aureus* and *E. coil*, respectively (Table 4). The reason for antimicrobial action may be due to their ability to absorb nutrients of bacteria and thus inhibition of bacterial growth or their interaction with negatively charged microbial cell membranes, resulting in increased permeability of the membranes. As shown in Figure 4, 6h-saponified nanocomposite particles possess a highly porous structure that can adsorb various ions and organic molecules easily in their pores and on their surfaces. Furthermore, bacterial growth or movement may be restricted by porous media physical conditions. Porosity networks with pore throat sizes narrower than the bacterial cell diameter prevent bacterial penetration into this region [23].

It is noted that the antibacterial activity against *S. aureus* and *E. coil* of the 6h-saponified nanocomposites decreased in order of EVA40/MWNT1200-6h > EVA28/MWNT1200-6h > PVAc/MWNT1200-6h whereas for unsaponified nanocomposites decreased in order of EVA28/MWNT1200 > EVA40/MWNT1200 > PVAc/MWNT1200. This indicated that there was an optimum VAc content for antibacterial activity against *S. aureus* and *E. coil*. EVA is a random copolymer consisting of ethylene and VAc as repeating units. VAc content has two fundamental effects that influence the properties of EVA copolymers. The first effect is to disrupt the crystalline regions formed by the polyethylene segments of the copolymer. The second overriding effect of VAc content results from the polar nature of the acetoxy side chain [24]. When the VAc group in polymer molecules converted to hydroxyl group through saponification, the total polarity of molecules is increased due to electronegativity of -OH group (2.68) is higher than that of VAc (2.56) one [25]. After saponification numerous hydroxyl groups in PVOH and EVOH form strong hydrogen bond, both inter- and intra-molecular, which reduce the free volume of the polymer chains. In case of EVA copolymers, the degree of hydrogen bonding can be controlled by varying ethylene and VOH ratios in the copolymer. This is the polarization of the -OH bonds, because the oxygen atoms are more electronegative than hydrogen atoms. However acetoxy group cannot form inter- and intra-molecular hydrogen bonds.

Tew and coworkers designed several aromatic oligomers based on arylamide [26], urea [27] and phenylene ethynylene [28] backbones. These aromatic oligomers have broad spectrum antimicrobial activity and selectivity. In the case of arylamides and ureas, rigidifying the conformation via hydrogen bonding which improved the antimicrobial activity. The phenylene ethynylene oligomers adopted a facially amphiphilic topology at the oil-water interface via proper placement of the amine groups and rotation around the single bonds [29]. They concluded that in the case of *S. aureus* while amphiphilicity is important, it is the overall hydrophobicity that determines their activity. For *E. coli*, antimicrobial activity was more sensitive to changes in amphiphilicity than *S. aureus*.

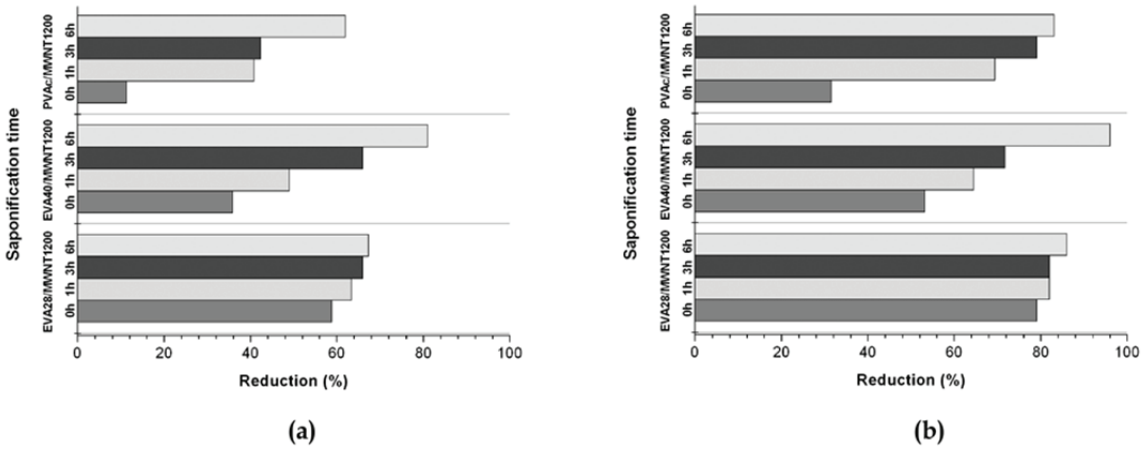

Fig. 4 Shake flask test results for the PVAc/MWNT1200, EVA40/MWNT1200, EVA28/MWNT1200 nanocomposite particles against S. aureus (a) and E. coli (b) as a function of saponification time.

In order to inactivate or kill microbes, the nanocomposite particles must come close to or touch the microbes. Such interactions are either attraction or repulsion. As most bacteria carry a net negative surface charge, adhesion of bacteria is discouraged on negatively charged surfaces, while it is promoted on positively charged surfaces [30, 31]. The increase in polarity of nanocomposites after saponification is reflected in the relative polar surface area, hydrogen bond donor, and hydrogen bond acceptor numbers, all of which increase substantially for antibacterial activity [32]. Furthermore all saponified nanocomposite particles inhibited the growth of *E. coli* more than *S. aureus* (Figure 9). Susceptibility differences between Gram positive and Gram negative bacteria may be due to cell wall structural differences between these classes of bacteria. The Gram negative bacterial cell wall outer membrane appears to act as a barrier to many substances, including synthetic and natural antibiotics [33]. The Gram-negative *E. coli* lipid membrane is richer in negative intrinsic curvature lipid phosphatidylethanolamine (～ 80%) as compared to the Gram-positive *S. aureus* lipid membrane. Thus, it is probable that disruption of Gram-negative bacteria requires more efficient hydrophobic components.

4. Conclusions

The antibacterial activity of the pristine MWNT and EB irradiated MWNT was compared against *S. aureus* and *E. coli* with the shake flask method. The MWNT was functionalized EB irradiation process in air with irradiation doses of 800, 1000, and 1200 kGy. After 24 h of bacterial contact, pristine MWNT extirpated 8.2 and 10.3 % of the viable cells of *S. aureus* and *E. coil*, respectively. With the EB irradiation dose the biological activity of MWNT was gradually increased. These functionalized MWNTs were dispersed in a VAc group containing polymer (PVA and EVA)/toluene solution and VOH group containing polymer (PVOH and EVOH)/MWNT nanocomposite particles were successfully prepared by direct precipitation and alkaline saponification. The nanocomposite particles have sponge-like structure of connected matrix polymer and MWNT fibres. As the saponification time increased the tensile properties of EVA40/MWNT1200 and EVA28/MWNT1200 were significantly increased. At 6h-saponification time, the tensile strength of EVA40/MWNT1200 nanocomposite was increased by 2.8-fold to 32.3 MPa whereas EVA28/MWNT1200 increased the tensile strength by 1.7-fold to 21.5 MPa as compared to the un-saponified one. The elongation at break of the both nanocomposite also increased by 1.6-fold and 5.2-fold, respectively. The tensile strength of PVAc/MWNT1200 nanocomposite significantly increased with saponification time. After 6h-saponification time, it enhanced by 222 %. However, the elongation at break of the PVAc/MWNT1200 almost remained same or has raised only maringally. This is indicated that saponification process enhances the overall dispersion state of the MWNT due to enhanced interactions between the filler and the polymer matrix. Similarly the antibacterial activity against both bacterial strains of all nanocomposites was gradually increased with the saponification time. The EVA40/MWNT1200-6h exhibited highest antibacterial activity against two strains. After 24 h of shaking, it showed 81 and 96 % inhibitions of the growth of *S. aureus* and *E. coil*, respectively. Materials with highly pore structure and controlled pore volume have potentials in a wide range of applications. Since the nanocomposite particles prepared by this method have highly porous, good mechanical properties and good antibacterial activity, they can be used for industrial applications such like antibacterial filler in coating system, antibacterial packaging film and antibacterial coating material.

References

[1] Zhou J, Qi X. Multi-walled carbon nanotubes/epilson-polylysine nanocomposite with enhanced antibacterial activityLetters in Applied Microbiology. 2010; 52:76-83.

[2] Saginur R, Stdenis M, Ferris W, Aaron SD, Chan F, Lee C, Ramotar K. Multiple combination bactericidal testing of staphylococcal biofilms from implant-associated infections. Antimicrobial Agents Chemother. 2006; 50:55-61.

[3] Pigrau C, Rodriguez-Pardo, MD. Infections associated with the use of indwelling urinary catheters. Infections related to intrauterine devices. Enfermedades Infecciosas y Microbiología Clínica. 2008; 26:299-310.

[4] Park ES, Kim HK, Shim JH, Kim MN, Yoon JS. Synthesis and properties of polymeric biocides based on poly ethylene-*co*-vinyl alcohol. Journal of Applied Polymer Science. 2004; 93:765-70.

[5] Park ES, Kim HS, Kim MN, Yoon JS. Antibacterial activities of polystyrene-*block*-poly(4-vinyl pyridine) and poly(styrene-*random*-4-vinyl pyridine). European Polymer Journal. 2004; 40:2819-22.

[6] Moon WS, Kim JC, Chung KH, Park ES, Kim, MN, Yoon, JS. Antimicrobial activity of a monomer and its polymer based on quinolone. Journal of Applied Polymer Science. 2003; 90:1797-801.

[7] Park, ES, Lee HJ, Park HY, Kim MN, Chung KH, Yoon JS. Antifungal effect of carbendazim supported on poly(ethylene-*co*-vinyl alcohol) and epoxy resin. Journal of Applied Polymer Science. 2001; 80:728-36.

[8] Park ES, Moon WS, Song MJ, Kim MN, Chung KH, Yoon JS. Antimicrobial activity of phenol and benzoic acid derivatives. International Biodeterioration & Biodegradation. 2001; 47:209-14.

[9] Park ES, Kim HK, Shim JH, Kim MN, Yoon JS. Synthesis and properties of polymeric biocides based on poly ethylene-*co*-vinyl alcohol. Journal of Applied Polymer Science. 2004; 93:765-70.

[10] Lewinski N, Colvin V, Drezek R. Cytotoxicity of nanoparticles. Small. 2008; 4:26-49.

[11] Kang S. Herzberg M. Rodrigues DF. Elimelech. Antibacterial Effects of Carbon Nanotubes: Size Does Matter!, Langmuir. 2008; 24:6409-13.

[12] Parker JR, Waddell WH. Quantitative characterization of polymer structure by photoacoustic Fourier transform infrared spectroscopy. Journal of Elastomers & Plastics. 1996; 28:140-60.

[13] Lau AKT, Hui D. The Revolutionary Creation of New Advanced Materials: Carbon Nanotube Composites, Composites Part B: Engineering. 2002; 33:263-67.

[14] Thostenson ET, Zhifeng R, Chou TW. Advances in the science and technology of carbon nanotubes and their composites: a review, Composite Science and Technology. 2001; 61:1899-912

[15] Burghard M, Balasubramanian K. Chemically Functionalized Carbon Nanotubes. Small, 2005; 2:180-92.

[16] Banhart F. Irradiation Effects in Carbon Nanostructures. Reports on Progress in Physics. 1999; 62:1181-221.

[17] Salvetat JP, Bonard JM, Thomson NH, Kulik AJ, Forro L, Benoit W, Zuppiroli L. Mechanical properties of carbon nanotubes, Applied Physics A. 1999; 69:255-60.

[18] Lee EJ, Yoon JS, Park ES. Preparation and Properties of the Highly Porous Poly(ethylene-*co*-vinyl alcohol)/Multiwalled Carbon Nanotube Nanocomposites Prepared by a Simple Saponification Method, Journal of Applied Polymer Science. 2012; 125: E691-E704.

[19] Lee EJ, Jeong HJ, Park ES. Antibacterial Activity of Highly Porous Vinyl Alcohol Group Containing Polymer/MWNT Nanocomposite Particles. American Chemical Society Division of Polymeric Materials: Science and Engineering. 2013; 108:2-3.

[20] Singh P, Tripathi RM, Saxena A. Synthesis of carbon nanotubes and their biomedical applications, Journal of Optoelectronics and Biomedical Materials. 2010; 2:91-8.

[21] Nel A, Xia T, Madler L, Li N. Toxic Potential of Materials at the Nanolevel, Science. 2006; 311:622-7.

[22] Jia G, Wang HF, Yan L, Wang X, Pei RJ, Yan T, Zhao YL, Guo XB. Cytotoxicity of Carbon Nanomaterials: Single-Wall. Nanotube, Multi-Wall Nanotube, and Fullerene, Environmental Science & Technology. 2005; 39:1378-83.

[23] Hazziza-Laskar J, Helary G, Sauvet G. Biocidal polymers active by contact. IV. Polyurethanes based on polysiloxanes with pendant primary alcohols and quaternary ammonium groups Journal of Applied Polymer Science. 1995; 58:77-84.

[24] George JJ, Bhowmick AK. Influence of Matrix Polarity on the Properties of Ethylene Vinyl Acetate-Carbon Nanofiller Nanocomposites. Nanoscale Research Letters. 2009; 4:655-64.

[25] Bratsch SG. A group electronegativity method with Pauling units. J. Chem. Edu.1966; 62:101-3.

[25] Tang H, Doerksen R, Jones T, Klein M, Tew G, Biomimetic Facially Amphiphilic Antibacterial Oligomers with Conformationally Stiff Backbones. Chemistry & Biology. 2006; 13:427-35.

[27] Tang H, Doerksen RJ, Tew GN. Synthesis of urea oligomers and their antibacterial activity. Chemical Communications. 2005; 28:1537-9.

[28] Arnt L, Rennie JR, Linser S, Willumeit R, Tew GN. Membrane activity of biomimetic facially amphiphilic antibiotics. Journal of Physical Chemistry B. 2006; 110: 3527-32.

[29] Arnt, L, Tew GN. Cationic facially amphiphilic poly(phenylene ethynylene)s studied at the air-water interface. Langmuir. 2003; 19:2404-8.

[30] Jucker BA, Harms H, Zehnder AB. Adhesion of the positively charged bacterium Stenotrophomonas (Xanthomonas) maltophilia 70401 to glass and Teflon. Journal of Bacteriology. 1996; 178:5472-79.

[31] Hogt AH, Dankert J and Feijen J. Adhesion of coagulase-negative staphylococci to methacrylate polymers and copolymers. Journal of Biomedical Materials Research. 1986; 20:533-45.

[32] Lee SS, Kim KR, Han SH, Jeong YS, Kim MN, Park ES. EVOH-based nanocomposites prepared by simple saponification method. Journal of Reinforced Plastics and Composites. 2001; 30:932-44.

[33] Singariya P. Kumar P, Mourya KK. Antibacterial and antifungal potential of some polar solvent extracts of Ashwagandha (Solanaceae) against the nosocomial pathogens. International Journal of Green Pharmacy. 2012; 6:17-22.

